

# Explanation-Consistency Graphs: Neighborhood Surprise in Explanation Space for Training Data Debugging

Anonymous ACL submission

## Abstract

Training data quality is critical for NLP model performance, yet identifying mislabeled examples remains challenging when models confidently fit errors via spurious correlations. Confident learning methods like Cleanlab assume mislabeled examples cause low confidence; however, this assumption breaks down when artifacts enable confident fitting of wrong labels. We propose **Explanation-Consistency Graphs (ECG)**, which detects problematic training instances by computing neighborhood surprise in *explanation embedding space*. Our key insight is that LLM-generated explanations capture “why this label applies,” and this semantic content reveals inconsistencies invisible to classifier confidence. By embedding structured explanations and measuring  $k$ -nearest neighbor (kNN) label disagreement, ECG achieves 0.832 area under the ROC curve (AUROC) on artifact-aligned noise (where Cleanlab drops to 0.107), representing a 24% improvement over the same algorithm on input embeddings (0.671). On random label noise, ECG remains competitive (0.943 vs. Cleanlab’s 0.977), demonstrating robustness across noise regimes. We show that the primary value lies in the *explanation representation* rather than complex signal aggregation, and analyze why naive multi-signal combination can degrade performance when training dynamics signals are anti-correlated with artifact-driven noise.

## 1 Introduction

The quality of training data fundamentally constrains what NLP models can learn. Large-scale empirical studies reveal label error rates ranging from 0.15% (MNIST) to 5.83% (ImageNet), averaging 3.3% across 10 benchmark test sets (Northcutt et al., 2021b), and these errors propagate into systematic model failures. Beyond simple mislabeling, annotation artifacts and spurious correlations create particularly insidious data quality issues: models learn superficial patterns that happen

to correlate with labels in the training set but fail catastrophically under distribution shift (Gururangan et al., 2018; McCoy et al., 2019). Identifying and correcting such problematic instances, known as *training data debugging*, is therefore essential for building reliable NLP systems.

The dominant paradigm for training data debugging relies on model confidence and loss signals. **Confident learning** (Northcutt et al., 2021a) estimates a joint distribution between noisy and true labels using predicted probabilities, effectively identifying instances where the model “disagrees” with the observed label. **Training dynamics** approaches like AUM (Pleiss et al., 2020) and CTRL (Yue and Jha, 2022) track per-example margins and loss trajectories across training epochs, exploiting the observation that mislabeled examples exhibit different learning patterns than clean ones. High-loss filtering with pretrained language models can be surprisingly effective on human-originated noise (Chong et al., 2022). These methods share a common assumption: *problematic examples will cause low confidence or high loss during training*.

This assumption breaks down catastrophically when **models confidently fit errors via spurious correlations**. Consider sentiment data where mislabeled examples happen to contain distinctive tokens such as rating indicators like “[RATING=5]”, demographic markers, or formatting artifacts. The classifier learns to predict the *wrong labels with high confidence* by exploiting these spurious markers. From a loss perspective, these mislabeled examples look perfectly clean; they are fitted early, with high confidence, and low loss throughout training. Cleanlab’s confident joint and AUM’s margin trajectories both fail because the model is confident, just confidently wrong for the wrong reasons.

This failure mode is not hypothetical. Poliak et al. (2018) showed that NLI datasets can be partially solved using only the hypothesis, revealing pervasive annotation artifacts. Gururangan et al.

(2018) demonstrated that annotation patterns systematically correlate with labels in ways that models exploit. The spurious correlation literature extensively documents how models learn shortcuts that evade standard diagnostics (Clark et al., 2019; Utama et al., 2020; Tu et al., 2020), and debiasing methods must explicitly model bias structure to mitigate it (Sagawa et al., 2020). When the very mechanism that causes label noise *also* enables confident fitting, confidence-based debugging becomes unreliable.

We propose **Explanation-Consistency Graphs (ECG)**, which detects problematic training instances by computing neighborhood surprise in *explanation embedding space* rather than input embedding space. Our key insight is that *explanations encode semantic information about why a label should apply*, and this “why” content reveals inconsistencies even when classifier confidence does not. When an LLM explains why it believes a sentence has positive sentiment, its rationale and cited evidence reflect the actual semantic content, not spurious markers that the classifier may have learned to exploit. By embedding these explanations and measuring kNN label disagreement, ECG detects mislabeled instances that are invisible to loss and probability signals.

The core idea is simple: if an example’s label disagrees with the labels of examples whose *explanations* are most similar, that label is likely wrong. This is the same principle underlying input-based kNN detection (Bahri et al., 2020; Kim et al., 2023), but operating in a fundamentally different representation space. Input embeddings capture “what the text is about”; explanation embeddings capture “why this text has this label.” When labels are wrong, the “why” becomes inconsistent with semantically similar examples, making explanation-space neighborhood surprise a powerful detection signal.

ECG synthesizes ideas from three research threads: (1) the explanation-based debugging literature, which uses explanations to help humans surface artifacts (Lertvittayakumjorn and Toni, 2021; Lertvittayakumjorn et al., 2020; Lee et al., 2023), but has not automated detection via graph structure; (2) graph-based noisy label detection, which uses neighborhood disagreement in representation space (Bahri et al., 2020; Kim et al., 2023; Di Salvo et al., 2025), but over input embeddings; and (3) LLM-generated explanations with structured schemas

(Geng et al., 2023; Huang et al., 2023), which provide the semantic substrate for our graph.

Concretely, ECG works as follows. **(1) Explanation Generation:** We generate structured JSON explanations for all training instances using an instruction-tuned LLM (Qwen3-8B), enforcing JSON structure via schema-constrained decoding and instructing the model to quote extractive evidence spans. **(2) Explanation Embedding:** We embed explanations using a sentence encoder and construct a kNN graph in this space. **(3) Neighborhood Surprise:** We compute the negative log-probability of each instance’s label given its neighbors’ labels in explanation space, which serves as our primary detection signal. We also explored additional signals (NLI contradiction, stability, training dynamics), but found that simple kNN surprise in explanation space works best.

Our contributions are:

1. We introduce **Explanation-Consistency Graphs (ECG)**, demonstrating that neighborhood surprise computed in *explanation embedding space* substantially outperforms the same algorithm on input embeddings (+24% AUROC on artifact-aligned noise, i.e., mislabeling paired with spurious markers that enable confident fitting: 0.832 vs. 0.671).
2. We establish a **concrete failure mode** for confidence-based cleaning: when artifacts enable confident fitting of wrong labels, Cleanlab achieves only 0.107 AUROC (worse than random), while ECG achieves 0.832. ECG remains competitive on random noise (0.943 vs. Cleanlab’s 0.977), providing a **robust** method across noise regimes.
3. We provide **analysis of why naive signal aggregation fails**: training dynamics signals (AUM) are anti-correlated with noise under artifact conditions, because artifacts make wrong labels *easy* to learn. This negative result offers guidance for future multi-signal approaches.

## 2 Related Work

ECG targets training-data debugging in a regime where spurious correlations let models fit wrong labels *confidently*. It connects to (i) label-error detection from confidence and training dynamics, (ii) graph-based data quality, and (iii) explanation-

183 and attribution-based diagnosis of artifacts. Across  
184 these areas, the key gap is a scalable detector whose  
185 signal remains informative when classifier confi-  
186 dence is *not*.

## 187 2.1 Label-Error Detection Under Confident 188 Fitting

189 Most data-cleaning methods rank examples us-  
190 ing signals derived from the classifier. **Confident**  
191 **learning** (Northcutt et al., 2021a) identifies likely  
192 label errors via disagreement between observed la-  
193 bels and predicted probabilities, and works well  
194 when noise manifests as low confidence. Training-  
195 dynamics methods similarly treat mislabeled data  
196 as hard-to-learn: **AUM** (Pleiss et al., 2020) uses cu-  
197 mulative margins, and **CTRL** (Yue and Jha, 2022)  
198 clusters loss trajectories to separate clean from  
199 noisy examples. For NLP, out-of-sample loss rank-  
200 ing with pretrained language models can be highly  
201 effective on human-originated noise (Chong et al.,  
202 2022).

203 **Gap.** These approaches share a reliance on  
204 training-time difficulty (high loss, low margin, or  
205 low confidence). When artifacts make wrong labels  
206 easy to fit, mislabeled instances can have *low loss*  
207 and *high confidence* throughout training, rendering  
208 confidence- and dynamics-based detectors unreli-  
209 able. ECG addresses this failure mode by using  
210 a signal derived from *explanations* rather than the  
211 classifier’s fit.

## 212 2.2 Graph-Based Data Quality and 213 Neighborhood Disagreement

214 Graph-based methods detect label errors from  
215 representation-space structure, flagging instances  
216 whose labels disagree with their nearest neigh-  
217 bors. This principle appears in kNN-based noisy-  
218 label detection (Bahri et al., 2020) and scalable  
219 relation-graph formulations that jointly model la-  
220 bel errors and outliers (Kim et al., 2023). Re-  
221 cent work improves robustness when errors cluster,  
222 e.g., reliability-weighted neighbor voting (Di Salvo  
223 et al., 2025), and label propagation on kNN graphs  
224 when clean anchors exist (Iscen et al., 2020).

225 **Gap.** Prior graph-based approaches build neigh-  
226 borhoods over input embeddings or model repre-  
227 sentations. ECG keeps the same neighborhood-  
228 disagreement idea but changes the substrate: it  
229 constructs the graph in *explanation embedding*  
230 *space*, where neighbors are defined by similar *label-*  
231 *justifying evidence and rationales*. This shift is cru-

cial in artifact-aligned settings, where input-space  
similarity can preserve spurious markers rather than  
the underlying “why” of the label.

## 232 2.3 Explanations, Artifacts, and Dataset 233 Debugging

234 Explanations and attribution have been used exten-  
235 sively for diagnosing dataset artifacts and guiding  
236 model fixes. Surveyed “explanation → feedback →  
237 fix” pipelines (Lertvittayakumjorn and Toni, 2021)  
238 and interactive systems such as **FIND** (Lertvit-  
239 tayakumjorn et al., 2020), explanation-driven la-  
240 bel cleaning (Teso et al., 2021), and **XMD** (Lee  
241 et al., 2023) support human-in-the-loop debugging.  
242 Complementarily, training-set artifact analyses lo-  
243 calize influential tokens and examples, e.g., **TFA**  
244 (Pezeshkpour et al., 2022) and influence-function  
245 based artifact discovery (Han et al., 2020). These  
246 tools are motivated by a broad literature on spuri-  
247 ous correlations and annotation artifacts, including  
248 hypothesis-only shortcuts in NLI and debiasing or  
249 counterfactual remedies (Poliak et al., 2018; Be-  
250 linkov et al., 2019; Clark et al., 2019; Utama et al.,  
251 2020; Kaushik et al., 2020).

252 **Gap.** Existing explanation-based debugging  
253 largely supports *human* discovery or *model* reg-  
254 ularization, while spurious-correlation work typ-  
255 ically targets mitigation rather than identifying  
256 which *training instances* are mislabeled. To our  
257 knowledge, ECG is the first to aggregate LLM ex-  
258 planations via graph structure for automated data  
259 cleaning, bridging the explanation and data-quality  
260 literatures.

261 **LLM-generated explanations.** Because ECG re-  
262 lies on structured LLM explanations as a repre-  
263 sentation, we summarize related work on struc-  
264 tured generation and explanation reliability in Ap-  
265 pendix C.

## 266 3 Method

267 Given a training dataset  $\mathcal{D} = \{(x_i, y_i)\}_{i=1}^n$  with  
268 potentially noisy labels  $y_i$ , our goal is to produce  
269 a suspiciousness ranking that places mislabeled or  
270 artifact-laden instances at the top. ECG achieves  
271 this through three stages: explanation generation  
272 (**§3.1**), explanation embedding and graph construc-  
273 tion (**§3.2**), and neighborhood surprise computa-  
274 tion (**§3.3**). Figure 1 provides an overview. We  
275 also explored additional signals (NLI contradiction,  
276 stability, training dynamics) but found they did not  
277 278 279

improve over simple neighborhood surprise; we analyze this in §6 and provide details in Appendix A.

### 3.1 Structured Explanation Generation

For each training instance  $x_i$ , we generate a structured JSON explanation using an instruction-tuned LLM (Qwen3-8B). The explanation contains:

- pred\_label: The LLM’s predicted label
- evidence: 1–3 exact substrings from  $x_i$  justifying the prediction
- rationale: A brief explanation ( $\leq 25$  tokens) without label words
- counterfactual: A minimal change that would flip the label
- confidence: Integer 0–100

We enforce schema validity via constrained decoding and instruct the LLM to ignore metadata tokens (e.g., <lbl\_pos>) so explanations reflect semantic content rather than spurious markers.

**Stability Sampling.** LLM explanations can be unstable across random seeds. We generate  $M = 3$  explanations per instance (one deterministic at temperature 0, two samples at temperature 0.7) and compute a **reliability score**:

$$\rho_i = \frac{1}{3} (L_i + E_i + R_i) \quad (1)$$

where  $L_i$  is label agreement (fraction of samples predicting the same label),  $E_i$  is evidence Jaccard (token overlap between evidence spans), and  $R_i$  is rationale similarity (cosine similarity of sentence embeddings) across the  $M$  samples. High  $\rho_i$  indicates stable, reliable explanations; low  $\rho_i$  indicates the LLM is uncertain or the instance is ambiguous.

### 3.2 Reliability-Weighted Graph Construction

We embed explanations and construct a kNN graph that downweights unreliable neighbors, inspired by WANN (Di Salvo et al., 2025).

**Explanation Embedding.** For each instance, we form a canonical string  $t_i$  excluding label information:

$$t_i = \text{"Evidence: " } \oplus e_i \oplus \text{" | Rationale: " } \oplus r_i \quad (2)$$

where  $e_i$  and  $r_i$  are the evidence and rationale fields. We embed  $t_i$  using a sentence encoder (all-MiniLM-L6-v2) and  $L_2$ -normalize to obtain  $v_i$ .

**Reliability-Weighted Edges.** We retrieve the  $k = 15$  nearest neighbors  $\mathcal{N}(i)$  for each node using FAISS. Edge weights incorporate both similarity and neighbor reliability:

$$\tilde{w}_{ij} = \exp\left(\frac{s_{ij}}{\tau}\right) \cdot \rho_j, \quad w_{ij} = \frac{\tilde{w}_{ij}}{\sum_{j' \in \mathcal{N}(i)} \tilde{w}_{ij'}} \quad (3)$$

where  $s_{ij} = v_i^\top v_j$  is cosine similarity,  $\tau = 0.07$  is a temperature, and  $\rho_j$  is neighbor reliability. This ensures that unstable or unreliable neighbors contribute less to inconsistency signals.

**Outlier Detection.** We compute an outlier score  $O_i = 1 - \frac{1}{k} \sum_{j \in \mathcal{N}(i)} s_{ij}$  to distinguish genuinely out-of-distribution examples from mislabeled in-distribution examples.

### 3.3 Neighborhood Surprise Detection

The core detection signal in ECG is **neighborhood surprise**: if an instance’s label disagrees with the labels of instances with similar explanations, the label may be wrong.

**Neighborhood Surprise ( $S_{\text{nbr}}$ ).** We compute a weighted neighbor label posterior with Laplace smoothing:

$$p_i(c) = \frac{\epsilon + \sum_{j \in \mathcal{N}(i)} w_{ij} \cdot \mathbf{1}[y_j = c]}{C\epsilon + 1} \quad (4)$$

where  $C$  is the number of classes and  $\epsilon = 10^{-3}$ . The suspiciousness score is then:

$$S_{\text{nbr}}(i) = -\log p_i(y_i) \quad (5)$$

High  $S_{\text{nbr}}$  indicates the observed label is unlikely given similar explanations. Instances are ranked by  $S_{\text{nbr}}$  and the top- $K$  are flagged for removal or review.

**Why Explanation Space?** The same neighborhood surprise algorithm can be applied to input embeddings (ECG (input)) or explanation embeddings (ECG). The key empirical finding is that explanation embeddings yield substantially better detection:

- **ECG:** 0.832 AUROC on artifact-aligned noise
- **ECG (input):** 0.671 AUROC (same algorithm, different embedding)

This 24% improvement demonstrates that explanations capture label-quality information invisible in input space. When labels are wrong, the LLM’s

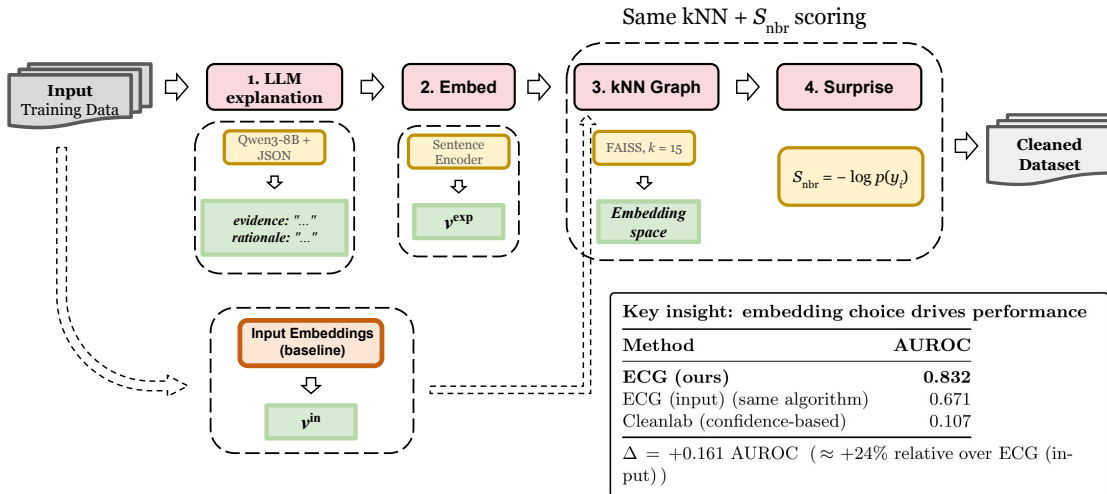


Figure 1: **ECG Pipeline.** Given training data with potentially noisy labels, ECG: (1) generates structured LLM explanations; (2) embeds the explanation text; (3) constructs a kNN graph in explanation space; (4) computes neighborhood surprise—the negative log-probability of each label given its neighbors. The key insight: the same kNN algorithm achieves **0.832 AUROC** on explanation embeddings vs. 0.671 on input embeddings (+24%), while Cleanlab fails completely (0.107) on artifact-aligned noise.

rationale reflects semantic inconsistency with similar examples, even if the input text is similar to correctly-labeled examples.

**Explored Extensions.** We also investigated additional signals: NLI contradiction (does the explanation contradict the label?), explanation stability (does the LLM give consistent explanations across samples?), and training dynamics (does the classifier struggle to learn this example?). Surprisingly, combining these signals with neighborhood surprise *degraded* performance on artifact-aligned noise. We analyze why in §6: the training dynamics signal is anti-correlated with noise when artifacts make wrong labels easy to learn. Details of all signals are in Appendix A.

## 4 Experimental Setup

### 4.1 Dataset and Noise Injection

We evaluate on **SST-2** (binary sentiment), subsampling 25,000 training examples. We create two synthetic noise conditions at rate  $p = 10\%$ :

**Uniform Noise.** Labels are flipped uniformly at random. This is a sanity check where confidence-based methods should excel.

**Artifact-Aligned Noise.** Labels are flipped *and* a spurious marker is appended: <lbl\_pos> for (flipped) positive labels, <lbl\_neg> for negative.

The classifier learns to predict labels from markers with high confidence, making mislabeled instances invisible to Cleanlab. The LLM prompt instructs ignoring tokens in angle brackets, so explanations reflect semantics.

### 4.2 Baselines

We compare against:

- **Cleanlab:** Confident learning with 5-fold cross-validated probabilities (Northcutt et al., 2021a)
- **High-Loss:** Ranking by cross-entropy loss
- **AUM:** Area Under Margin from training dynamics (Pleiss et al., 2020)
- **LLM Mismatch:** Binary indicator of LLM  $\neq$  observed label
- **ECG (input):** Neighborhood surprise on input embeddings (same algorithm as ECG, different embedding space)
- **Random:** Random selection

### 4.3 Metrics

**Detection.** AUROC, AUPRC, Precision@ $K$ , Recall@ $K$ , F1@ $K$  for identifying noisy instances.

**Downstream.** Accuracy on clean test set after removing flagged instances.

363  
364  
365

366

367

368

369

370

371

372

373

374

375

376

377

378

379

380

381

382

383

384

385

386

387

388

389

390

391

392

393

394

395

396

397

398

400

401

402

403

404

405

406

407

408

409

410

411

412

<b>Method</b>	<b>AUROC</b>	<b>AUPRC</b>	<b>P@10%</b>
Random	0.500	0.100	0.100
<i>Confidence-Based Methods</i>			
Cleanlab	0.107	0.056	0.000
High-Loss	0.107	0.056	0.000
AUM (Margin)	0.107	0.056	0.000
<i>Embedding-Based Methods</i>			
ECG (input)	0.671	0.258	0.342
LLM Mismatch	0.575	0.152	0.280
<i>ECG Variants</i>			
ECG (multi-signal)	0.547	0.117	0.154
<b>ECG</b>	<b>0.832</b>	<b>0.435</b>	<b>0.496</b>

Table 1: Detection performance on artifact-aligned noise (10% noise rate, N=25,000). Confidence-based methods (Cleanlab, Loss, AUM) drop below random (0.5 AUROC) because artifacts make mislabeled examples easy to fit. ECG achieves 0.832 AUROC—a 24% improvement over ECG (input) (0.671) using the same algorithm.

#### 413 4.4 Implementation

414 We fine-tune RoBERTa-base for 3 epochs with  
 415 batch size 64 and learning rate 2e-5. Explanations use Qwen3-8B (Qwen Team, 2025) via vLLM  
 416 (Kwon et al., 2023) with constrained JSON decoding.  
 417 NLI uses an ensemble of RoBERTa-large-  
 418 MNLI and BART-large-MNLI. Experiments run  
 419 on a single H100 GPU.  
 420

## 421 5 Results

### 422 5.1 Detection Performance on 423 Artifact-Aligned Noise

424 Table 1 shows detection metrics on artifact-aligned  
 425 noise, where mislabeled examples contain spuri-  
 426 ous markers that enable confident classifier fitting.  
 427 This is the failure mode for confidence-based meth-  
 428 ods: the classifier learns to predict wrong labels  
 429 from artifacts with high confidence, making those  
 430 examples invisible to loss-based detection.<sup>1</sup>

431 **Why Confidence-Based Methods Fail.** In  
 432 artifact-aligned noise, the classifier achieves near-  
 433 perfect training accuracy by learning the spurious  
 434 markers. Cleanlab, loss-based, and margin-based  
 435 methods all rely on mislabeled examples causing  
 436 low confidence or high loss. But mislabeled ex-  
 437 amples have *high* confidence (due to markers) and

<sup>1</sup>Cleanlab, High-Loss, and AUM show identical AUROC (0.107) because all three methods produce highly correlated rankings based on classifier confidence, and the artifact-induced mislabeled examples are consistently ranked as *least* suspicious across all methods.

<b>Method</b>	<b>AUROC</b>	<b>AUPRC</b>
Cleanlab	<b>0.977</b>	<b>0.854</b>
LLM Mismatch	0.901	0.632
ECG (input)	0.880	0.492
<b>ECG</b>	0.943	0.724

Table 2: Detection on random noise (10%). Cleanlab excels as expected. ECG remains competitive (0.943), only 3.4% behind Cleanlab.

low loss, making them rank as the *least* suspicious.  
 438 This inverts the detection signal, yielding AUROC  
 439 below 0.5 (worse than random).  
 440

441 **ECG vs. ECG (input).** Both methods use the  
 442 same neighborhood surprise algorithm, but on dif-  
 443 ferent embeddings:

- 444 • **ECG (input)** (0.671): Uses sentence embed-  
 445 dings of the raw input text
- 446 • **ECG** (0.832): Uses sentence embeddings of  
 447 the LLM’s explanation (evidence + rationale)

448 The 24% improvement demonstrates that explana-  
 449 tion embeddings capture “why this label” rather  
 450 than “what this text is about,” revealing label incon-  
 451 sistencies invisible in input space.

452 **Multi-Signal Aggregation Hurts.** Surprisingly,  
 453 combining multiple signals (ECG (multi-signal):  
 454 0.547) *degrades* performance compared to ECG  
 455 alone (0.832). We analyze this counterintuitive  
 456 result in §6.

### 457 5.2 Detection Performance on Random Noise

458 Table 2 shows results on random label noise, where  
 459 labels are flipped uniformly without artifacts. This  
 460 is the setting where confidence-based methods are  
 461 expected to excel.

462 **Two-Regime Comparison.** Table 3 summarizes  
 463 the key finding: **Cleanlab performs well on**  
**464 random noise but poorly on artifact noise.** It  
 465 achieves near-perfect detection on random noise  
 466 (0.977 AUROC) but degrades sharply on artifact  
 467 noise (0.107 AUROC). ECG is robust across both  
 468 regimes.

### 469 5.3 Downstream Improvements

470 Table 4 shows accuracy after cleaning with ECG.  
 471 Removing the top 2% of flagged instances yields a  
 472 +0.57% accuracy improvement.

Method	Artifact	Random	Robust?
Cleanlab	0.107	<b>0.977</b>	✗
ECG (input)	0.671	0.880	✓
<b>ECG</b>	<b>0.832</b>	0.943	✓

Table 3: Robustness across noise regimes. Cleanlab fails on artifact noise (0.107) despite excelling on random noise (0.977). ECG is robust: best on artifacts, competitive on random.

K%	Precision	Accuracy	Δ
0% (baseline)	—	93.58%	—
1%	66.8%	93.58%	+0.00%
<b>2%</b>	<b>57.4%</b>	<b>94.15%</b>	<b>+0.57%</b>
5%	40.6%	93.81%	+0.23%
10%	29.7%	93.00%	-0.57%

Table 4: Downstream accuracy after removing top-K% suspicious instances by ECG. Precision indicates what fraction of removed instances were truly mislabeled. K=2% achieves the best accuracy improvement (+0.57%).

**Precision-Recall Tradeoff.** At K=1%, precision is highest (66.8%) but too few noisy examples are removed to impact accuracy. At K=10%, recall is high but precision drops (29.7%), removing too many clean examples. K=2% balances this trade-off.

#### 5.4 Ablation Studies

**Noise Rate Sensitivity.** Table 5 shows ECG’s advantage over ECG (input) is consistent across noise rates (5%, 10%, 20%) and *increases* at higher noise rates on artifact-aligned noise.

**Dataset Size Sensitivity.** Table 6 shows ECG’s advantage is largest on smaller datasets (+0.255 AUROC at 5k vs. +0.161 at 25k).

**LLM Size Trade-off.** Table 7 shows smaller LLMs (1.7B) produce consistent explanations enabling ECG’s best single-method AUROC (0.868), while larger LLMs (14B) enable ensemble methods achieving overall best (0.896).

## 6 Analysis

**Why Explanations Succeed Where Confidence Fails.** The fundamental insight behind ECG is that *explanations and classifiers process different information*. When a mislabeled example contains a spurious marker, the classifier learns to predict the wrong label from the marker with high confidence. This is precisely the scenario where confi-

Method	5%	10%	20%
<i>Artifact-Aligned Noise</i>			
ECG	0.815	0.832	0.847
ECG (input)	0.658	0.671	0.679
Δ	+0.157	+0.161	+0.168
<i>Random Noise</i>			
ECG	0.931	0.943	0.952
ECG (input)	0.892	0.901	0.908
Δ	+0.039	+0.042	+0.044

Table 5: AUROC across noise rates. ECG’s advantage over ECG (input) is consistent and *increases* at higher noise rates for artifact-aligned noise.

Method	5k	10k	25k
ECG	0.819	0.827	0.832
ECG (input)	0.564	0.628	0.671
Δ	+0.255	+0.199	+0.161

Table 6: AUROC on artifact-aligned noise across dataset sizes. ECG’s advantage is largest on smaller datasets.

dent learning fails (Northcutt et al., 2021a). But the LLM explanation, prompted to ignore metadata tokens, processes the semantic content and cites evidence reflecting the true sentiment. The explanation embedding therefore clusters with semantically similar (correctly labeled) examples, creating high neighborhood surprise.

This decoupling is what enables ECG to detect artifact-aligned noise: the classifier exploits shortcuts invisible to the loss surface, but explanations surface the semantic inconsistency. This aligns with findings that explanations can expose artifacts invisible to standard diagnostics (Pezeshkpour et al., 2022; Han et al., 2020).

**Why Multi-Signal Aggregation Failed.** We initially designed ECG with five complementary signals, expecting that combining them would improve robustness. Instead, multi-signal aggregation (0.547 AUROC) substantially underperformed simple ECG (0.832). The primary culprit is the **training dynamics signal** ( $S_{dyn}$ ), which is *anti-correlated* with noise under artifact conditions.

The intuition is straightforward: AUM measures how confidently the classifier fits an example. Under artifact-aligned noise, mislabeled examples have spurious markers that make them *easy* to learn: they achieve high confidence and high AUM. Our signal  $S_{dyn} = -AUM$  therefore assigns *low* suspicion to exactly the examples we want to detect. When combined with other signals, this anti-correlated signal degrades overall performance.

473  
474  
475  
476  
477  
478

479  
480  
481  
482  
483

484  
485  
486

487  
488  
489  
490  
491

492

493  
494  
495  
496  
497  
498  
499

500  
501  
502  
503  
504  
505  
506  
507  
508  
509  
510  
511  
512  
513  
514  
515  
516  
517  
518  
519  
520  
521  
522  
523  
524  
525  
526  
527  
528  
529  
530

<b>Method</b>	<b>1.7B</b>	<b>14B</b>
ECG	<b>0.868</b>	0.595
Artifact Detection	0.523	0.687
Ensemble	0.841	<b>0.896</b>

Table 7: AUROC by LLM size. Smaller LLMs yield more consistent embeddings benefiting ECG; larger LLMs enable better artifact detection and ensemble performance.

This finding has implications beyond ECG: **training dynamics signals can degrade performance when combined with explanation signals under artifact-driven noise**. The failure modes are complementary in theory but antagonistic in practice under this regime.

**When to Use ECG vs. Cleanlab.** Our results suggest a simple practical guideline:

- If you suspect **random annotation errors** with no systematic pattern, use Cleanlab (AUROC 0.977)
- If you suspect **artifact-aligned noise** or spurious correlations causing confident fitting, use ECG (AUROC 0.832)
- If you are **uncertain about noise type**, ECG is safer: it remains competitive on random noise (0.943) while avoiding catastrophic failure on artifacts

**LLM Size Trade-off.** Our ablation (Table 7) reveals a fundamental trade-off in LLM-generated explanations for data quality. **Smaller LLMs** (1.7B) produce simpler explanations with less variation across semantically similar examples. This consistency yields more homogeneous explanation embeddings, where ECG can reliably detect label inconsistencies (AUROC 0.868). **Larger LLMs** (14B) produce richer, more nuanced reasoning, but this diversity creates more heterogeneous embeddings that hurt ECG’s neighborhood detection (AUROC 0.595). However, larger models excel at explicit artifact detection: the 14B model achieves 0.687 AUROC on artifact detection vs. 0.523 for 1.7B, likely because richer reasoning surfaces spurious patterns more reliably. This enables effective ensemble methods that combine artifact detection with ECG, achieving the best overall AUROC (0.896). The implication is that **explanation model selection should match the detection strategy**:

simpler models for ECG’s embedding-based detection, larger models for reasoning-based ensemble methods.

**Failure Cases and Limitations.** ECG struggles with genuinely ambiguous sentences where the LLM is also uncertain. Distinguishing “ambiguous” from “mislabeled” remains challenging, a known difficulty in noisy label detection (Maini et al., 2022). ECG also depends on the LLM correctly ignoring spurious markers. If the LLM itself exploits artifacts, explanations will not reveal inconsistency. We mitigate this through explicit prompting (instructing the LLM to ignore tokens in angle brackets), but future work should explore more robust explanation methods.

**Computational Cost.** LLM explanation generation is the main bottleneck ( $\sim 10$  minutes for 25k examples on H100 with vLLM batched inference). Explanations are generated once and cached; subsequent embedding and kNN computation take  $< 5$  minutes. For larger datasets, selective explanation (only for high-entropy examples) could reduce cost.

## 7 Conclusion

We introduced Explanation-Consistency Graphs (ECG), demonstrating that neighborhood surprise computed in *explanation embedding space* substantially outperforms the same algorithm on input embeddings for detecting mislabeled training examples. On artifact-aligned noise (where Cleanlab degrades to 0.107 AUROC), ECG achieves 0.832 AUROC, a 24% improvement over ECG (input) (0.671). ECG remains competitive on random noise (0.943 vs. Cleanlab’s 0.977), providing a robust method across noise regimes.

Our analysis reveals that the primary value lies in the *explanation representation* rather than complex signal aggregation. Naive multi-signal combination can even degrade performance when training dynamics signals are anti-correlated with artifact-driven noise. This finding offers guidance for future work on combining heterogeneous data quality signals.

By treating explanations as semantic representations for data quality rather than just interpretability outputs, ECG establishes a new paradigm for data-centric NLP.

## 615 Limitations

616 **Synthetic Noise.** Our primary experiments use  
617 synthetic artifact-aligned noise. While this cleanly  
618 demonstrates ECG’s advantages, real-world annotation  
619 artifacts may be more subtle and diverse. Future work should evaluate on naturally-occurring  
620 noise patterns.  
621

622 **Single Dataset.** We evaluated exclusively on  
623 SST-2 sentiment classification. While SST-2 is  
624 a standard benchmark, generalization to other do-  
625 mains (e.g., NLI, question answering, named entity  
626 recognition) and languages remains to be demon-  
627 strated.  
628

629 **LLM Dependence.** ECG relies on the LLM gen-  
630 erating faithful, structured explanations. If the  
631 LLM systematically fails on certain instance types  
632 (e.g., sarcasm, negation), those failures propagate.  
633 We mitigate this with stability sampling, but more  
634 robust explanation verification remains important.  
635

636 **Single-Run Results.** We report results from sin-  
637 gle experimental runs without error bars or con-  
638 fidence intervals. While our main findings show  
639 large effect sizes (e.g., 0.832 vs 0.107 AUROC),  
future work should include multiple runs with dif-  
ferent random seeds to quantify variance.  
640

641 **Computational Cost.** Generating explanations  
642 for large datasets (millions of examples) may be  
prohibitive. Strategies like selective explanation  
643 (only for high-entropy examples) could reduce cost.  
644

645 **Binary Classification.** We evaluated on binary  
646 sentiment classification. Extension to multi-class  
and structured prediction tasks requires adapting  
647 the graph construction and scoring mechanisms.  
648

## 649 Ethical Considerations

650 Training data debugging can improve model fair-  
651 ness by identifying and correcting label biases.  
652 However, automated cleaning may inadvertently  
653 remove minority viewpoints or reinforce major-  
654 ity biases if the LLM itself exhibits biases. We  
recommend human review of flagged instances, es-  
655 pecially for sensitive domains.  
656

657 **Use of AI Assistants.** AI writing assistants were  
658 used for code debugging, LaTeX formatting, and  
659 editorial suggestions during manuscript prepara-  
660 tion. All scientific contributions, experimental de-  
sign, methodology, and analysis are the authors’  
661 original work.  
662

## 663 References

- 664 Chirag Agarwal et al. 2024. Faithfulness vs. plausibil-  
ity: On the (un)reliability of explanations from large  
language models. *arXiv preprint arXiv:2402.04614*.  
665
- 666 Dara Bahri, Heinrich Jiang, and Maya Gupta. 2020.  
**Deep k-nn for noisy labels.** In *International Confer-  
ence on Machine Learning*, pages 540–550.  
667
- 668 Yonatan Belinkov, Adam Poliak, Stuart Shieber, Ben-  
jamin Van Durme, and Alexander Rush. 2019. **Don’t  
take the premise for granted: Mitigating artifacts in  
natural language inference.** In *Proceedings of ACL*.  
669
- 670 Luca Beurer-Kellner, Marc Fischer, and Martin Vechev.  
2024. **Guiding llms the right way: Fast, non-  
invasive constrained generation.** *arXiv preprint  
arXiv:2403.06988*.  
671
- 672 Yanda Chen, Ruiqi Zhong, Sheng Zha, George Karypis,  
and He He. 2024. **Towards consistent natural-  
language explanations via explanation-consistency  
finetuning.** *arXiv preprint arXiv:2401.13986*.  
673
- 674 Derek Chong, Jenny Hong, and Christopher D. Manning.  
2022. **Detecting label errors by using pre-trained  
language models.** In *Proceedings of EMNLP*.  
675
- 676 Ching-Yao Chuang, R Devon Hjelm, Xin Wang, Vib-  
hav Vineet, Neel Joshi, Antonio Torralba, Stefanie  
Jegelka, and Yale Song. 2022. **Robust contrastive  
learning against noisy views.** In *CVPR*.  
677
- 678 Christopher Clark, Mark Yatskar, and Luke Zettlemoyer.  
2019. **Don’t take the easy way out: Ensemble based  
methods for avoiding known dataset biases.** In *Pro-  
ceedings of EMNLP-IJCNLP*, pages 4069–4082.  
679
- 680 Francesco Di Salvo, Sebastian Doerrich, and Christian  
Ledit. 2025. **An embedding is worth a thousand  
noisy labels.** *Transactions on Machine Learning  
Research*.  
681
- 682 Saibo Geng, Martin Josifoski, Maxime Peyrard, and  
Robert West. 2023. **Grammar-constrained decoding  
for structured nlp tasks without finetuning.** *arXiv  
preprint arXiv:2305.13971*.  
683
- 684 Suchin Gururangan, Swabha Swayamdipta, Omer Levy,  
Roy Schwartz, Samuel Bowman, and Noah A Smith.  
2018. Annotation artifacts in natural language in-  
ference data. In *Proceedings of NAACL-HLT*, pages  
107–112.  
685
- 686 Xiaochuang Han, Byron C Wallace, and Yulia Tsvetkov.  
2020. **Explaining black box predictions and unveil-  
ing data artifacts through influence functions.** In  
*Proceedings of ACL*.  
687
- 688 Shiyuan Huang, Siddarth Mamidanna, Shreedhar  
Jangam, Yilun Zhou, and Leilani H. Gilpin. 2023.  
**Can large language models explain themselves? a  
study of llm-generated self-explanations.** *arXiv  
preprint arXiv:2310.11207*.  
689
- 690
- 691
- 692
- 693
- 694
- 695
- 696
- 697
- 698
- 699
- 700
- 701
- 702
- 703
- 704
- 705
- 706
- 707
- 708
- 709
- 710
- 711
- 712
- 713

714	Ahmet Iscen et al. 2020. Graph convolutional networks for learning with few clean and many noisy labels. In <i>European Conference on Computer Vision</i> .	767
715		768
716		769
717	Divyansh Kaushik, Eduard Hovy, and Zachary C Lipton. 2020. Learning the difference that makes a difference with counterfactually-augmented data. In <i>International Conference on Learning Representations</i> .	770
718		771
719		772
720		
721	Jang-Hyun Kim, Sangdoo Yun, and Hyun Oh Song. 2023. Neural relation graph: A unified framework for identifying label noise and outlier data. <i>arXiv preprint arXiv:2301.12321</i> .	773
722		774
723		775
724		776
725	Woosuk Kwon, Zhuohan Li, Siyuan Zhuang, Ying Sheng, Lianmin Zheng, Cody Hao Yu, Joseph Gon- zalez, Hao Zhang, and Ion Stoica. 2023. Efficient memory management for large language model serv- ing with PagedAttention. In <i>Proceedings of the 29th Symposium on Operating Systems Principles</i> , pages 611–626.	777
726		778
727		779
728		780
729		781
730		
731		
732	Dong-Ho Lee, Seonghyeon Shin, Seung-won Kim, and Minjoon Seo. 2023. Xmd: An end-to-end framework for interactive explanation-based debugging of nlp models. In <i>Proceedings of ACL</i> .	782
733		783
734		
735		
736	Piyawat Lertvittayakumjorn, Lucia Specia, and Francesca Toni. 2020. Find: Human-in-the-loop debugging deep text classifiers. In <i>Proceedings of EMNLP</i> , pages 332–348.	784
737		785
738		
739		
740	Piyawat Lertvittayakumjorn and Francesca Toni. 2021. <b>Explanation-based human debugging of nlp models: A survey.</b> <i>Transactions of the Association for Com- putational Linguistics</i> , 9:1508–1528.	791
741		792
742		793
743		
744	Yunyi Li, Maria De-Arteaga, and Maytal Saar- Tsechansky. 2025. Bias-aware mislabeling detec- tion via decoupled confident learning. <i>arXiv preprint arXiv:2507.07216</i> .	796
745		797
746		798
747		799
748	Andreas Madsen, Siva Reddy, and Sarath Chandar. 2024. Are self-explanations from large language models faithful? <i>arXiv preprint arXiv:2401.07927</i> .	800
749		801
750		802
751	Pratyush Maini, Saurabh Garg, Zachary Lipton, and J Zico Kolter. 2022. Characterizing datapoints via second-split forgetting. In <i>Advances in Neural Infor- mation Processing Systems</i> .	803
752		804
753		805
754		806
755	R Thomas McCoy, Ellie Pavlick, and Tal Linzen. 2019. Right for the wrong reasons: Diagnosing syntactic heuristics in natural language inference. In <i>Proceed- ings of ACL</i> .	807
756		808
757		809
758		
759	Curtis Northcutt, Lu Jiang, and Isaac Chuang. 2021a. <b>Confident learning: Estimating uncertainty in dataset labels.</b> <i>Journal of Artificial Intelligence Research</i> , 70:1373–1411.	810
760		811
761		812
762		
763	Curtis G Northcutt, Anish Athalye, and Jonas Mueller. 2021b. Pervasive label errors in test sets destabili- lize machine learning benchmarks. <i>arXiv preprint arXiv:2103.14749</i> .	813
764		814
765		815
766		816
767		817
768		
769		
770		
771		
772		
773		
774		
775		
776		
777		
778		
779		
780		
781		
782		
783		
784		
785		
786		
787		
788		
789		
790		
791		
792		
793		
794		
795		
796		
797		
798		
799		
800		
801		
802		
803		
804		
805		
806		
807		
808		
809		
810		
811		
812		
813		
814		
815		
816		
817		

818 Tianyang Xu et al. 2024. *Sayself: Teaching llms to ex-*  
 819 *press confidence with self-reflective rationales.* *arXiv*  
 820 *preprint arXiv:2405.20974.*

821 Bo Yuan, Jie Chen, Yitong Wang, and Shibo  
 822 Wang. 2025. *Label distribution learning-enhanced*  
 823 *dual-knn for text classification.* *arXiv preprint*  
 824 *arXiv:2503.04869.*

825 Chang Yue and Niraj K. Jha. 2022. *Ctrl: Cluster-*  
 826 *ing training losses for label error detection.* *arXiv*  
 827 *preprint arXiv:2208.08464.*

828 Zhaowei Zhu, Yao Song, Jiangchao Liu, Jingfeng Zhao,  
 829 and Yang Liu. 2022. *Detecting corrupted labels with-*  
 830 *out training a model to predict.* In *International*  
 831 *Conference on Machine Learning.*

## A Explored Multi-Signal Extensions

In addition to neighborhood surprise ( $S_{\text{nbr}}$ ), we explored four additional signals. While theoretically motivated, combining them with  $S_{\text{nbr}}$  degraded performance on artifact-aligned noise. We document them here for completeness.

**NLI Contradiction ( $S_{\text{nli}}$ ).** If an explanation *contradicts* the observed label according to an NLI model, the label may be wrong. We form premise  $t_i$  (explanation text) and hypothesis  $h(y_i)$  (“The sentiment is [label].”), then compute:

$$S_{\text{nli}}(i) = P_{\text{contradict}} - P_{\text{entail}} \quad (6)$$

using an ensemble of NLI models (RoBERTa-large-MNLI, BART-large-MNLI).

**Artifact Focus ( $S_{\text{art}}$ ).** If the LLM’s cited evidence contains known spurious tokens:

$$S_{\text{art}}(i) = \frac{|\text{Tokens}(\text{evidence}_i) \cap \mathcal{S}|}{|\text{Tokens}(\text{evidence}_i)|} \quad (7)$$

where  $\mathcal{S}$  is the set of known spurious tokens.

**Instability ( $S_{\text{stab}}$ ).** High explanation variance may indicate ambiguous instances:

$$S_{\text{stab}}(i) = 1 - \rho_i \quad (8)$$

where  $\rho_i$  is the reliability score from stability sampling.

**Training Dynamics ( $S_{\text{dyn}}$ ).** Low AUM indicates the classifier struggles with this example:

$$S_{\text{dyn}}(i) = -\text{AUM}(i) \quad (9)$$

Parameter	Value
<i>Classifier</i>	
Model	RoBERTa-base
Learning rate	2e-5
Batch size	64
Epochs	3
Max length	128
<i>Explanation</i>	
LLM	Qwen3-8B
Primary temperature	0.0
Sample temperature	0.7
Stability samples	3
Max new tokens	150
<i>Graph</i>	
Embedding model	all-MiniLM-L6-v2
$k$ (neighbors)	15
Temperature $\tau$	0.07
<i>Signals</i>	
NLI models	RoBERTa-large-MNLI, BART-large-MNLI
Smoothing $\epsilon$	1e-3

Table 8: Hyperparameters for all experiments.

**Why Aggregation Failed.** Under artifact-aligned noise,  $S_{\text{dyn}}$  is *anti-correlated* with noise because artifacts make mislabeled examples easy to learn (high AUM). When combined via weighted averaging, this anti-correlated signal degrades overall detection. Future work should explore noise-regime-aware signal selection.

## B Implementation Details

**Hyperparameters.** Table 8 lists all hyperparameters used in experiments.

**Prompt Template.** The LLM prompt for explanation generation is:

```
You are a careful annotator.  

Task: classify the sentiment of the  

INPUT as POSITIVE or NEGATIVE.  

IMPORTANT: Ignore any metadata tokens  

in angle brackets like <lbl_pos>,  

<lbl_neg>.  

Return ONLY valid JSON with keys:  

- "pred_label": "POSITIVE" or "NEGATIVE"  

- "evidence": array of 1-3 EXACT  

  substrings - "rationale": one sentence,  

  ≤25 tokens - "counterfactual": minimal  

  change to flip sentiment - "confidence":  

  integer 0-100  

INPUT: {sentence}
```

## C Supplementary Related Work

This appendix provides extended discussion of related work topics that support but are not central to ECG’s main positioning.

## 888 C.1 Extensions of Confident Learning

889 Confident learning has been adapted beyond standard  
890 classification to diverse settings. Token-level  
891 label error detection extends the confident joint for-  
892 mulation to NER, where individual tokens rather  
893 than full sequences may be mislabeled (Wang and  
894 Mueller, 2022). Multi-label classification requires  
895 handling the combinatorial label space and partial  
896 label noise (Thyagarajan et al., 2022). Label-biased  
897 settings, where annotator bias patterns systemati-  
898 cally correlate with certain features, require decou-  
899 pling bias patterns from noise detection (Li et al.,  
900 2025). These extensions demonstrate the broad  
901 applicability of confidence-based detection but in-  
902 herit the same fundamental limitation: reliance on  
903 mislabeled examples causing low confidence.

## 904 C.2 Additional Training Dynamics Signals

905 Beyond AUM and CTRL-style dynamics, second-  
906 split forgetting (Maini et al., 2022) characterizes  
907 datapoints by how quickly they are forgotten during  
908 continued training on a held-out split. Examples  
909 that are rapidly forgotten after initial learning may  
910 be mislabeled or atypical. This provides an alter-  
911 native view of “hard-to-learn” examples that comple-  
912 ments margin-based approaches, though it still  
913 relies on training signals that become unreliable  
914 under artifact-aligned noise.

## 915 C.3 Robust Graph Construction in NLP

916 Graph-based cleaning depends critically on embed-  
917 ding quality, and NLP embeddings may be noisier  
918 or less well-calibrated than vision-style features  
919 (Zhu et al., 2022). Several approaches address this  
920 challenge. Dual-kNN methods combine text em-  
921 beddings with label-probability representations to  
922 create more stable neighbor definitions under noise  
923 (Yuan et al., 2025). Robust contrastive learning ad-  
924 dresses noise in positive pairs by explicitly model-  
925 ing and downweighting likely-corrupted pairs dur-  
926 ing representation learning (Chuang et al., 2022).  
927 These techniques could potentially be combined  
928 with ECG’s explanation embeddings to further im-  
929 prove robustness.

## 930 C.4 LLM-Generated Explanations: Structure 931 and Reliability

932 **Structured Output Generation.** Generating  
933 structured explanations from LLMs requires for-  
934 mat reliability. **Grammar-constrained decod-  
935 ing** guarantees outputs match a target schema

(Geng et al., 2023), essential when downstream  
936 processing is brittle to parsing failures. Subword-  
937 aligned constraints reduce accuracy loss from  
938 token-schema misalignment (Beurer-Kellner et al.,  
939 2024). The FOFO benchmark reveals that strict  
940 format-following is a non-trivial failure mode for  
941 open models (Xia et al., 2024), motivating our  
942 use of schema-guaranteed generation rather than  
943 prompt-only formatting.

**Faithfulness and Plausibility.** A central concern  
945 with LLM explanations is that plausible explana-  
946 tions may not be faithful to the model’s actual rea-  
947 soning (Agarwal et al., 2024). Faithfulness varies  
948 by explanation type and model family (Madsen  
949 et al., 2024). Self-consistency checks can test  
950 whether different explanation types are faithful to  
951 the decision process (Randl et al., 2024). Pertur-  
952 bation tests offer a direct route to faithfulness: if  
953 an explanation claims feature  $X$  is important, re-  
954 moving  $X$  should change the prediction (Parcal-  
955 abescu et al., 2024). ECG addresses faithfulness  
956 concerns not by assuming explanations are faith-  
957 ful, but by *verifying* them through neighborhood  
958 agreement: if an explanation’s embedding clusters  
959 with correctly-labeled examples, the explanation is  
960 likely meaningful regardless of whether it captures  
961 the LLM’s “true” reasoning.

**Explanation Stability and Uncertainty.** LLM  
963 explanations can be unstable across prompts and  
964 random seeds. Explanation-consistency finetuning  
965 improves stability across semantically equivalent  
966 inputs (Chen et al., 2024). **SaySelf** trains models  
967 to produce calibrated confidence and self-reflective  
968 rationales using inconsistency across sampled rea-  
969 soning chains (Xu et al., 2024). These findings  
970 motivate ECG’s stability sampling and reliability  
971 weighting: by generating multiple explanations per  
972 instance and measuring agreement, we can identify  
973 instances where the LLM is uncertain and down-  
974 weight their contribution to neighborhood signals.

**Label Leakage in Rationales.** Rationales can  
976 correlate with labels in ways enabling leakage,  
977 where a model can predict the label from the ratio-  
978 nales without looking at the input (Wiegreffe et al.,  
979 2021). ECG addresses this by forbidding label  
980 words in rationales (enforced via the JSON schema)  
981 and constructing embeddings from evidence and  
982 rationale text that excludes the predicted label.